BEHAVIOUR AND ANALYTICAL MODELS OF REINFORCED CONCRETE COLUMNS UNDER BIAXIAL EARTHQUAKE LOADS

Shunsuke Otani, V. Wai-To Cheung and Shing Sham Lai

SYNOPSIS

The effect of biaxial lateral loading on the hysteretic behaviour of reinforced concrete columns is studied through laboratory experiment. No axial load was applied to the specimens in order to simplify the experiment. Three pairs of columns have been tested. One column of each pair was tested under uniaxial lateral loading, while the other under biaxial lateral load reversals.

Diagonal cracks, flexural cracks, crushing and spalling of shell concrete was observed on all four faces of the biaxially loaded columns. The final failure modes of a pair of specimens were quite similar. Loading and resulting damage in the transverse direction reduced the stiffness of a biaxially loaded column in the longitudinal direction. However, the overall hysteretic characteristics of a pair of uniaxially and biaxially loaded columns were similar. The degrading trilinear hysteresis model simulates favourably the hysteretic behaviour of biaxially loaded columns.

RESUME

Des résultats expérimentaux sur le comportement biaxial des colonnes en béton armé sont présentés. Trois paires de colonnes, dont une chargée latéralement dans une direction et l'autre chargée dans deux directions orthogonales, sont à l'étude. Aucune charge axiale est appliquée. Les modes de ruine pour les deux colonnes de chaque paire sont similaires, même si la rigidité dans la direction principale était diminuée pour les membres chargés biaxiallement. Un modèle mathématique à trois droites représente convenablement le comportement hystérétique des colonnes en régime biaxial en tenant compte d'une variation de la résistance résiduelle.

S. Otani is associate professor of Civil Engineering, University of
Toronto. Dr. Otani's research interests include nonlinear behaviour
of the reinforced concrete, earthquake engineering and structural
dynamics.

V. W.-T. Cheung is a graduate student in the Department of Civil
Engineering, University of Toronto. Mr. Cheung received a B.A.Sc.
degree from the University of Toronto.

S.S. Lai is a graduate student in the Department of Civil Engineering,
University of Toronto. Mr. Lai obtained a B.E.Sc. degree from the
University of Western Ontario, and a M.Eng. degree from the University
of Toronto.

INTRODUCTION

The earthquake motion is not limited to one horizontal direction.
In fact, the National Building Code of Canada 1977 (1) requires the
minimum lateral seismic force to be assumed to act non-concurrently in
any horizontal direction. However, independent design about each of
the principal axes together with the associated torsional forces is
considered to provide adequate resistance against earthquake motions
applied in any direction (2).

If a structure is provided with regularly placed shear walls in
the two perpendicular directions, the routine design analysis may be
justifiable because the stiffness and strength of a shear wall in the
longitudinal direction are much higher than those in the transverse
direction. On the other hand, columns of a framed structure must re-
sist lateral forces in two directions, simultaneously. Therefore, a
column must be designed for possible combinations of biaxial bending
moments and shear forces in addition to the vertical axial load. If
damage in a column caused by motion in one direction reduces the re-
sisting capacity of the column in the transverse direction, then the
safety of the structure is not warranted.

It is desirable to design a frame structure so that plastic
hinges would form only at the beam ends during an earthquake because a
large amount of hysteretic energy is expected to dissipate at a beam
end through ductile flexural deformation beyond yielding without jeo-
pardizing the safety of the structure. However, the moment at the
base of a first storey column is inevitably large, and it is difficult
to prevent yielding at the base of the first storey column. Therefore,
it is necessary to study the behaviour of a first storey column under
biaxial lateral load reversals well into the inelastic range.

The methods to estimate the strength of reinforced concrete
column sections under monotonically increasing compression and biaxial
bending have been studied by many investigators on the basis of
flexural theory, for example (3,4), and on the basis of static

experiments to failure, for example (5,6). However, the strength and deformability under "monotonically increasing loads" are not sufficient performance criteria of the reinforced concrete under earthquake motion because the oscillation causes stress reversals and because the stiffness and ductility of the reinforced concrete depend on a load history. Therefore, it is necessary to examine if a reinforced concrete column can resist design axial load, biaxial bending moments and shears when the column is subjected to a probable seismic loading history including loading reversals.

Innumerable experiments have been carried out on reinforced concrete columns subjected to axial load and uniaxial lateral load reversals. Observations on earthquake damaged structures and accompanying analyses of the damage (7,8) triggered recent experimental studies on the behaviour of reinforced concrete members under biaxial lateral load reversals (9,10,11). These experimental studies revealed a significant reduction in resistance and stiffness due to biaxial lateral load reversals.

Some effort has been made to analyze structures subjected to biaxial horizontal earthquake motions (12-17). Most have assumed either the elasto-plastic or the bilinear hysteretic model in the analysis of a simple reinforced concrete column or a frame structure. The basic effects of bilinear-biaxial interaction on the earthquake response (12,14,15) are that, (a) the horizontal biaxial ground motion increased ductility demand for stiff structures, and that (b) the horizontal biaxial motion had little effect on the ductility demand of flexible structures. However, if the effect of stiffness degradation is included in the biaxial interaction hysteretic properties of a structural model (13,16), the maximum displacements can be significantly increased from those of the non-degrading biaxial hysteresis models such as elasto-plastic and bilinear systems.

In order to improve the reliability and accuracy of the nonlinear dynamic analysis, it is essential to develop realistic hysteretic models for a reinforced concrete column. The objective of this study is, (a) to study the effect of biaxial lateral loading on the hysteretic behaviour of reinforced concrete, and (b) to examine the applicability of different hysteretic models in simulating reinforced concrete behaviour under lateral load reversals.

OUTLINE OF EXPERIMENTAL WORK

The behaviour of reinforced concrete columns subjected to a series of static biaxial lateral load reversals was studied. The test specimens represented a portion of a first storey column between the foundation and the inflection point of the column. No axial load was applied to the specimens in order to simplify the experiment. Three pairs of columns have been tested. Each pair of columns was constructed using the same materials and specifications. An odd-numbered column of each pair was tested under uniaxial lateral load reversals, and an even-numbered specimen under biaxial lateral load reversals. The same dimensions were used in all six columns as shown in Fig. 1. The amount of longitudinal and lateral reinforcement and the strength

of concrete were varied in the three pairs of test columns. The properties of the concrete and the reinforcement are listed in Table 1.

The longitudinal reinforcement in specimens SP-1 & 2 was welded to a grid made of four 76 x 610 x 9.5-mm steel plates at 51 mm below the top face of the footing so that the deformation attributable to the slippage of the longitudinal reinforcement within the footing is minimized. In this manner, it was expected that the deformation characteristics of the column portion could be separated from the complex interactive behaviour of the column-footing assemblage. However, the column specimens failed by the fracture of the longitudinal reinforcement at this very location of welding. Consequently, the longitudinal reinforcement was welded to the grid at the base of the footing in the subsequent specimens (Fig. 1).

The arrangement of longitudinal and transverse reinforcement is shown in Fig. 1. In specimens SP-1 & 2, three different shape ties, made of No. 3 bars, were placed at the same level with a uniform interval of 127 mm. Square ties made of No. 3 bars in specimens SP-3 & 4 were welded at the splice and then heat treated. The spacing of the ties over a length equal to twice effective depth from the footing surface was approximately one-quarter effective depth, and the spacing was doubled outside this region. In specimens SP-5 & 6, the tie bar was extended at least 76 mm beyond the 135° bend. The spacing was uniform over the column height.

The shear resisting capacities as evaluated by the ACI Standard 318-77 (18) using a capacity reduction factor are 2.3, 1.6, and 1.1 times the shear corresponding to the calculated flexural capacity (without capacity reduction factor) for specimens SP-1 & 2, SP-3 & 4, and SP-5 & 6, respectively. Specimens SP-3 & 4 had a higher shear resistance capacity near the column base than the value quoted above.

The footing was fastened to the test platform by eight 44.5-mm diameter high strength bolts. The loading system for biaxial lateral loading is schematically shown in Fig. 2. Two servo-controlled 220-kN actuators were used to apply translational displacement in NS direction. A manually-controlled reversible ram (142-kN capacity) was used in EW direction. The details of the loading system and instrumentation are described in Reference (19).

Typical loading programs used for specimens SP-5 & 6 are shown in Fig. 3. The deflections are expressed in terms of the ratio of applied deflection to a calculated yield deflection. The yielding of a section was defined by the tensile yielding of the second layer reinforcement (not the bottom layer reinforcement) from the extreme tensile fibre of the section under monotonically increasing load in a principal direction. Only flexural deformation was considered in calculating the yielding deflection.

The following principles were applied in determining the loading program: (a) displacement was applied only in one principal direction within one cycle of loading reversal so that the behaviour in the two orthogonal directions could be compared with the behaviour under

uniaxial lateral load reversals; (b) at least two cycles of displacement reversal were applied whenever the displacement amplitude exceeded the previous maximum amplitude. The two cycles were necessary to examine if the hysteresis loop was stable under load reversals; (c) before increasing the displacement amplitude, one cycle at a small displacement amplitude was applied to study the stiffness characteristics. During an earthquake motion, such small- to medium-amplitude oscillations occur between large-amplitude oscillations. Therefore, it is important that a hysteretic model includes hysteretic rules for such cases.

OBSERVED BEHAVIOUR

General Observation

All specimens developed flexural cracks in concrete mostly at the tie levels, diagonal shear cracks, both along the entire height of a column, followed by tensile yielding of the longitudinal reinforcement, and compressive crushing of concrete at the base of the columns.

X-shaped diagonal shear cracks appeared on all four faces of the biaxially loaded specimens, whereas diagonal cracks appeared on the two faces parallel to the loading direction in the uniaxially loaded specimens. Similarly, crushing and spalling of shell concrete was observed on all four faces of the biaxially loaded specimens. Splitting cracks along longitudinal reinforcement were also observed toward the end of a test (Fig. 4).

Although diagonal cracks were observed on the column faces, the behaviour of the specimens was dominated by flexure. The deterioration in stiffness and resistance due to shear "pinching" in the hysteresis was not detected until the last stage in the test.

Specimens SP-1 and SP-2 failed by the fracture of longitudinal reinforcement at a location where a piece of metal was accidentally welded near the critical section. Later tension tests of coupon bars showed that the fracture strain of bars with a welded metal piece was approximately 1%, whereas the fracture strain of bars without welding was approximately 9%. An innocent welding on a reinforcing bar during construction can significantly reduce the ductility of a structure. The maximum displacement amplitudes obtained in specimens SP-1 and SP-2 were 4.1 and 3.0 times the calculated yield displacement, respectively. Although crushing and light surface spalling of the concrete were observed at the base of the two columns, the concrete appeared sound at the time of failure.

Failure of specimens SP-3 and SP-4 was due to buckling of the longitudinal bars near the base after spalling of the shell concrete and extensive cracking and crumbling of the core concrete. The concrete within the reinforcement cage was so disintegrated by diagonal shear cracking, grinding along the diagonal cracks and flexural cracking, the crumbled concrete pieces could be removed by fingers toward the end of the tests. The shear resisting capacity outside twice effective depth from the footing face was more than 1.5 times the shear

corresponding to the calculated ultimate moment at the base. Further-more, the spacing of ties was reduced to one-half in the critical region. Such heavy lateral reinforcement resulted in the maximum ob-served displacement of the specimens SP-3 and SP-4 to be as much as 8.2 and 9.8 times the calculated yield displacement, respectively.

Specimens SP-5 and SP-6 had the least shear resisting capacity of the three specimens. After separation and spalling of shell concrete outside the longitudinal reinforcement cage, the core concrete was also broken into pieces due to flexural cracks, crushing of concrete and diagonal shear cracks. The resistance of the two specimens was lost through the disintegration of the core concrete. The shell con-crete (concrete outside the tie reinforcement) spalled off over a length equal to twice effective depth from the footing surface. The maximum displacements observed were 4.8 times the calculated yield displacement for the two specimens. Figure 4 shows crack patterns ob-served in specimens SP-5 and SP-6 at approximately the same damage. The crushing of concrete, spalling of shell concrete, diagonal shear cracks and splitting cracks were observed on all four faces in bi-axially loaded specimen SP-6.

The last four specimens (SP-3 through SP-6) were provided with the same amount of longitudinal reinforcement, whereas the lateral re-inforcement ratio of SP-3 & 4 was more than twice that of SP-5 & 6. By far smaller ductility of specimens SP-5 & 6 must be mainly attri-butable to the difference in the amount of lateral reinforcement at the critical region provided in the two pairs of specimens. In order to increase the ductility of a reinforced concrete column, it is important to provide sufficient amount of tie reinforcement in the critical region so that the core concrete can be held tight even after crushing and shear cracking of the concrete.

The lower ductility of specimens SP-5 & 6 might have been also attributable to the lower concrete compressive strength in those two specimens, causing the longitudinal reinforcement ratio closer to the balanced reinforcement ratio of the section.

Load-Deflection Relationship Under Uniaxial Loading

Lateral deflections at the point of loading were measured by ± 127-mm linear variable differential transformers. As the measured deflections included the footing movement, the deflections were cor-rected for the rigid body translation and rotation of the footing using the measured footing deflection (rotation and translation).

The stiffness of a test specimen decreased with increasing damage and load reversals. A typical force-deflection curve obtained from test SP-5 is shown in Fig. 5. The load was applied in only NS direction. The observations can be summarized as follows:

(a) Stiffness changed due to flexural cracking of concrete and tensile yielding of the longitudinal reinforcement;

(b) When a deflection reversal was repeated at the same newly

attained maximum amplitude, the stiffness in the second cycle was noticeably lower than that in the first cycle, although the resistances at the peak displacement were almost identical. In Fig. 5, the displacement amplitude in cycle 3 was repeated in cycle 4. Note a distinct reduction in stiffness in load cycle 4, and also note comparable resistances at the maximum displacement in these two cycles. This reduction in stiffness is attributable to the formation of additional cracks during the loading in cycle 3, and also attributable to a reduced stiffness of the longitudinal reinforcement in cycle 4 due to the Bauschinger effect;

(c) Average stiffness (peak-to-peak) of a complete cycle decreases with a previous maximum displacement amplitude. For example, after the specimen being subjected to large amplitude displacement reversals in cycles 3 and 4, the peak-to-peak stiffness of cycle 5 is significantly reduced from that of cycle 2, although the displacement amplitudes of cycles 2 and 5 were comparable. The peak-to-peak stiffness in cycle 5 was close to that in cycles 3 and 4;

(d) Therefore, the hysteretic characteristics of the reinforced concrete are dependent on the loading history.

Effect of Transverse Loading

The behaviour of specimen 4, subjected to biaxial loading, is examined to study the effect of transverse loading on the hysteretic characteristics. The tensile yielding of longitudinal reinforcement was observed in cycle 12 in NS direction. After loading cycle 13, repeating the same amplitude as in cycle 12, the forced displacement was applied in EW direction, causing first yielding in EW direction in cycle 16. The displacement amplitudes in cycle 12 (NS) and cycle 16 (EW) were comparable. Note that the stiffness in cycle 16 is much less than that in cycle 12. This stiffness reduction was attributable to the damage caused by loading in NS direction.

After two displacement reversals (cycles 19 and 20) at an amplitude 4.5 times the calculated yield displacement as shown in Fig. 6(b), the specimen was subjected to a forced displacement reversal (cycle 22) in NS direction at the amplitude used in cycle 13 (previous maximum amplitude in NS direction). The stiffness in cycle 22 was significantly reduced from the stiffness in cycle 13 as demonstrated by a dashed line in Fig. 6(a). This stiffness reduction is a direct result of damage caused during loading in the transverse loading. Note that subsequent loading cycles 23 and 24 did not show a sign of failure.

Does the biaxial lateral load reversal cause a substantial stiffness reduction which may not be detected by a uniaxial lateral load reversal test? The force-deflection relation curves observed during tests on specimens SP-5 and SP-6 are compared for this purpose. Both specimens were subjected to the same number of load cycles and also similar displacement histories as shown in Fig. 3. Figure 7(a) shows the force-deflection curves of specimen SP-5. The hysteresis loops in NS and EW directions of specimen SP-6 are combined and plotted in Fig. 7(b). The general shapes of the two curves in Fig. 7(a) and (b)

are quite similar, indicating the hysteretic characteristic obtained through uniaxial lateral load reversals can provide a good index to judge the performance under biaxial lateral load reversals as long as the behaviour is dominantly flexural. Specimen SP-5 failed at a smaller deflection amplitude than specimen SP-6. The larger maximum load was obtained from specimen SP-6.

The rotation was measured at the base of each column specimen over a distance approximately equal to the effective depth of section. The moment-rotation relationships also indicated the hysteretic character-istics similar to the ones observed from the force-deflection relation-ships.

HYSTERETIC MODELS FOR UNIAXIAL LOADING

Some effort has been made to analyze structures subjected to bi-axial horizontal earthquake motions. In some studies, the stiffness characteristics of the reinforced concrete section or member under a multi-axial stress state have been represented by simple unrealistic models (12,14,15), or extrapolated from the stiffness characteristics under a uniaxial stress state through various hypotheses of the theory of plasticity (16). It is necessary to study the applicability of such hypotheses or simple hysteresis models in simulating the behaviour of the reinforced concrete under stress reversals.

The capability of four representative hysteresis models in simu-lating the observed hysteretic behaviour of a reinforced concrete column under uniaxial lateral load reversals is first examined. These models are, (a) bilinear model, (b) Clough's degrading stiffness model (20), (c) Takeda model (21), and (d) degrading trilinear model (22). All four models provide resistance history corresponding to a given displacement history. The model parameters are defined by a backbone curve which is a force-deflection relation under monotonically in-creasing load, and which is normally idealized by a bilinear or tri-linear curve.

The basic stiffness properties (cracking, yielding and ultimate points) under monotonically increasing load were determined by the geo-metry of the test structure, and by the material properties found from standard material tests. The cracking point was defined as a load stage at which the extreme tensile fibre stress reached the splitting tensile strength of the concrete. The yielding was defined by the tensile yielding of the second layer of reinforcement from the extreme tensile fibre. After yielding, the curvature was assumed to distri-bute uniformly over the already yielded region. The ultimate point was taken as a point where the maximum resistance was developed in calculation. Only flexural deformation was considered. The shear de-formation and deformation attributable to slippage of the longitudinal reinforcement within the footing were not considered. Therefore, cal-culated displacements at the three points are inevitably smaller than the actual displacements observed during a test. The hysteresis models were subjected to the displacement history observed during test SP-5 under uniaxial lateral load reversals (Figs. 8-13). Note that the com-puted resistance (used by the models) was larger than the observed

resistance after yielding.

Bilinear Model

The model assumes a bilinear backbone curve, and its stiffness is elastic whenever the stress is between negative and positive yield stresses. Upon yielding, the stiffness is reduced to a fraction of the elastic stiffness. Figure 8 compares the performance of a bilinear model with the observed column behaviour. Note that the bilinear hysteresis model is not sufficient to simulate the basic behaviour of the specimen. The bilinear model does not dissipate hysteretic energy until yielding is developed. However, once yielding develops, the bilinear hysteresis loop becomes much larger than the observed hysteresis loop. Therefore, the performance of a bilinear model is not satisfactory for the simulation of reinforced concrete behaviour.

Clough Model

This model also assumes a bilinear backbone curve. During loading, the response point always moves toward the previous maximum response point. Once the previous maximum displacement is exceeded, yielding is assumed. The unloading stiffness is always the same as the elastic one. Figure 9 compares the performance of a Clough model with the observed behaviour. Although the flexural cracking is ignored, the correlation is generally good as long as the displacement amplitude is greater than the yield value. However, when the displacement amplitude is less than the yield value, a good performance cannot be expected from this model.

Takeda Model

A hysteresis model, similar to the Clough model, was developed independently by Takeda, Sozen and Nielsen (21). The model includes the stiffness changes due to flexural cracking and yielding. Unloading stiffness after yielding is reduced by an exponential function of previous maximum deformation. The model also includes a set of rules for load reversals at displacement amplitude less than previous peak amplitudes. Figures 10 and 11 compare the performance of Takeda models with the observed behaviour. The exponent to define the unloading stiffness was suggested to be a value of 0.5 (Fig. 10) in the original work (21). The correlation is not good in this case. Therefore, the exponent was arbitrarily changed to a value of 0.1 (Fig. 11). The correlation is improved significantly, especially for hysteresis loops beyond yielding. However, the value of the exponent could not be determined on a rational basis from the geometry of the test structure and the properties of the materials. The shape of large-amplitude hysteresis loops of the Takeda model is almost identical to that of the Clough model.

Degrading Trilinear Model

A simple hysteresis model was developed by a Japanese research group (22). The model assumes a trilinear backbone curve. Up to "yielding", the model behaves in the same manner as the bilinear model.

Once deformation exceeds the yield point, the model response follows the backbone curve. Upon unloading from the maximum response point on the backbone curve, the unloading point is treated as a new yield point. The unloading stiffnesses are reduced so that the behaviour becomes the same as the bilinear model in a range between the positive and negative "yield" points. In other words, the stiffness of a bilinear hysteresis is gradually degraded with a peak displacement amplitude beyond yielding.

Figures 12 and 13 compare the performance of degrading trilinear models with the observed behaviour. When the first stiffness change point is defined as the flexural cracking point (Fig. 12), the performance of the model is not satisfactory because the area of a hysteresis loop becomes too small. Therefore, the first stiffness change point was arbitrarily defined by extending initial uncracked stiffness to a force level equal to one-third flexural yield force. In this case, the performance is improved significantly as shown in Fig. 13. This indicates that the cracking (first stiffness change) point of the degrading trilinear model should not be taken as the actual cracking point, but rather the point should be used to control the fatness of a hysteresis loop. However, further studies need be carried out in order to determine the parameters of a degrading trilinear model on a rational basis.

Summary

The bilinear model is not sufficient to simulate the behaviour of reinforced concrete. The Clough model is relatively simple, but the performance is good especially when the displacement amplitude is greater than the yield value. The Takeda model and the degrading trilinear model are good if the parameters are properly chosen.

HYSTERETIC MODEL FOR BIAXIAL LOADING

The development of analytical methods and rapid progress in the study of nonlinear behaviour of reinforced concrete members and sub-assemblies have made it feasible to discuss the nonlinear behaviour of reinforced concrete plane structures with a certain confidence. However, we have not reached a point to discuss nonlinear behaviour of three-dimensional building structures, partly because reliable hysteresis models for the reinforced concrete under biaxial lateral load reversals are not available.

Although a uniaxial bilinear hysteretic model can be easily extended to a biaxial hysteretic model through the application of Prager's kinematic hardening theory modified by Ziegler (23), the bilinear model does not simulate the behaviour of the reinforced concrete under reversed loading. The Clough model and the Takeda model are more difficult to extend in a two-force domain because the stiffness change occurs when the sign of stress changes. On the other hand, the performance of the degrading trilinear model is essentially a bilinear type. Therefore, the degrading trilinear model can be adapted in a biaxial loading case as demonstrated by Takizawa and Aoyama (16) making use of various hypotheses of the theory of plasticity (23,24,25). Let

us examine the performance of the biaxial degrading trilinear model following the development by Takizawa and Aoyama (16).

The biaxial degrading trilinear model consists of two similar ellipses, corresponding to "cracking" and "yielding" surfaces in a biaxial force plane. Although the inner ellipse is called a "cracking" ellipse, the actual role of the inner ellipse is to control the range of straight unloading portion as demonstrated in Figs. 12 and 13 in the uniaxial loading case. Therefore, the cracking (inner) ellipse is chosen to be similar in shape to the yielding (outer) ellipse. The initial values for "cracking" do not correspond to the actual flexural cracking load of a specimen, but rather are arbitrarily chosen to be one-third of the calculated yield forces in the current analysis.

When a response force point lies within the inner ellipse, the behaviour of the model is linearly elastic, as shown in Fig. 14(a), until the point touches the cracking ellipse; i.e., cracking. When cracking occurs, the response point lies on the inner ellipse and moves with the inner ellipse within the yielding ellipse as shown in Fig. 14(b). The cracking ellipse is not allowed to move outside the yield ellipse. When the inner ellipse touches the outer ellipse, the cracking ellipse must slide along the yielding ellipse as shown in Fig. 15. Once the response point on the inner ellipse touches the outer ellipse, the yielding of the model is assumed to occur. The yielding ellipse expands in size, showing the strain hardening and stiffness degradation effects of the model. The inner ellipse expands in size proportional to the outer ellipse size. The shape of the cracking and yielding ellipses must remain similar to the original ones. The stiffness degradation is related to the increase in size of the yielding ellipse.

The goodness of this model was examined by subjecting the model to the biaxial displacement history observed during test SP-6. The force-deflection curves of the test specimen and the hysteretic models are compared in Fig. 16. The general behaviour of the test specimen is simulated favourably by the hysteretic model particularly with the fact that lineal lines are used in the model to approximate the real curved stiffness. The initial stiffness and yield points were evaluated by the flexural theory on the basis of the geometry and material . properties. The biaxial degrading trilinear model represented major trends of the test specimen in the two orthogonal directions.

A study by Takizawa and Aoyama (16) on single-mass models under horizontal biaxial ground motion concluded that the effect of biaxial response interaction on the maximum earthquake response is generally very significant for the biaxial degrading type model, while the effect is not so important for the non-degrading type model. The current experimental study on the reinforced concrete column supports previous findings (9,10,11) that there exists a pronounced biaxial interaction, causing a stiffness degradation in a principal direction due to damage in the transverse direction. Therefore, the maximum response of a reinforced concrete structure under biaxial horizontal earthquake motion can be much greater than the maximum response computed by subjecting the structural model to one component of

earthquake motion at a time.

CONCLUDING REMARKS

The effect of biaxial lateral loading on the hysteretic behaviour of reinforced concrete columns was experimentally investigated. Under biaxial lateral loading, diagonal cracks, flexural cracks, crushing and spalling of shell concrete was observed on all four faces of a column before failure.

The final modes of failure of a pair of identically constructed columns were similar subjected to either uniaxial or biaxial lateral load reversals. The overall hysteretic characteristics of such a pair of columns were quite similar.

Loading and resulting damage in the transverse direction reduced significantly the stiffness of a biaxially loaded column.

The "degrading" trilinear hysteresis model simulates major dominantly-flexural behaviour of uniaxially and biaxially loaded reinforced concrete columns.

ACKNOWLEDGMENT

LIST OF REFERENCES

1. Associate Committee on the National Building Code, <u>National Building Code of Canada, 1977</u>, National Research Council of Canada, Ottawa, 1977.

2. Associate Committee on the National Building Code, "Commentaries on Part 4 of the National Building Code of Canada 1977", National Research Council of Canada, Ottawa, 1977, Commentary J.

3. Pannell, F.N., "The Design of Biaxially Loaded Columns by Ultimate Load Methods", Magazine of Concrete Research, London, Vol. 12, No. 35, July 1960, pp. 99-108.

4. Furlong, R.W., "Ultimate Strength of Square Columns Under Biaxially Eccentric Loads", Journal, American Concrete Institute, Vol. 57, No. 9, March 1961, pp. 1129-40.

5. Bresler, B., "Design Criteria for Reinforced Columns Under Axial Load and Biaxial Bending", Journal, American Concrete Institute, Proceedings, Vol. 57, No. 5, Nov. 1960, pp. 481-490.

6. Ramamurthy, L.N., "Investigation of the Ultimate Strength of Square and Rectangular Columns Under Biaxially Eccentric Loads", Publication SP-13, Symposium on Reinforced Concrete Columns, American Concrete Institute, 1966, pp. 263-298.

7. Okada, T., et al, "Analysis of the Hachinohe Library Damaged by 1968 Tokachi-Oki Earthquake", Proceedings, U.S.-Japan Seminar on Earthquake Engineering, Sendai, September 1970, pp. 172-189.

8. Ersoy, O.K., Selna, L.G. and Morrill, K.B., "Shear Failure, Elastic and Inelastic Analyses of the Olive View Hospital Psychiatric Day Clinic: A Study of Causes of Failure and Remedies for Survival", Report, Earthquake Engineering and Structures Laboratory, University of California at Los Angeles, May 1973.

9. Okada, T., Seki, M. and Asai, S., "Response of Reinforced Concrete Columns to Bi-Directional Horizontal Force and Constant Axial Force", Bulletin of Earthquake Resistant Structure Research Centre, The Institute of Industrial Science, University of Tokyo, No. 10, December 1976, pp. 30-36.

10. Takiguchi, K. and Kokusho, S., "Hysteretic Behaviours of Reinforced Concrete Members Subjected to Bi-Axial Bending Moments", Proceedings, Sixth World Conference on Earthquake Engineering, New Delhi, India, Jan. 1977, Session 11, p. 250.

11. Maruyama, K., Ramirez, H. and Jirsa, J.O., "Behaviour of Reinforced Concrete Columns Under Biaxial Lateral Loading", Proceedings, Sixth European Conference on Earthquake Engineering, Dubrovnik, Yugoslavia, Sept. 1978, pp. 135-141.

12. Nigam, N.C., "Inelastic Interaction in the Dynamic Response of Structures", Ph.D. Thesis, California Institute of Technology, Pasadena, 1967.

13. Aktan, A.E., Pecknold, D.A.W. and Sozen, M.A., "Effect of Two-Dimensional Earthquake Motion on a Reinforced Concrete Column", Structural Research Series No. 399, University of Illinois, Urbana, May 1973.

14. Padilla-Mora, R. and Schnobrich, W.D., "Non-linear Response of Framed Structures to Two-Dimensional Earthquake Motion", SRS No. 408, University of Illinois, Urbana, July 1974.

15. Pecknold, D.A.W., "Inelastic Structural Response to 2D Ground Motion", Journal, Engineering Mechanics Division, ASCE, Vol. 100, No. EM5, October 1974, pp. 949-963.

16. Takizawa, H. and Aoyama, H., "Biaxial Effects in Modelling Earthquake Response of R/C Structures", Journal, Earthquake Engineering and Structural Dynamics, John Wiley and Sons, Ltd., Vol. 4, 1976, pp. 523-552.

17. Selna, L.G. and Lawder, J.H., "Biaxial Inelastic Frame Seismic Behaviour", Reinforced Concrete Structures in Seismic Zones, ACI, Publication SP-53, 1977, pp. 439-461.

18. American Concrete Institute, "Building Code Requirements for Reinforced Concrete", Standard ACI 318-77, Detroit, 1977.

19. Otani, S. and Tang, C.S., "Behaviour of Reinforced Concrete Columns Under Biaxial Lateral Load Reversals - (I) Pilot Test -", Publication 78-03, University of Toronto, Toronto, February 1978.

20. Clough, R.W., "Effect of Stiffness Degradation on Earthquake Ductility Requirements", Report 66-16, Structures and Materials Research, University of California, Berkeley, October 1966.

21. Takeda, T., Sozen, M.A. and Nielsen, N.N., "Reinforced Concrete Response to Simulated Earthquakes", Journal, Structural Division, ASCE, Vol. 96, December 1970, pp. 2557-73.

22. Fukada, Y., "Study on the Restoring Force Characteristics of Reinforced Concrete Buildings (in Japanese)", Proceedings, Kanto District Symposium, Architectural Institute of Japan, No. 40, 1969.

23. Ziegler, H., "A Modification of Prager's Hardening Rule", Quarterly, Applied Mathematics, Vol. 17, No. 1, April 1959, pp. 55-65.

24. Hill, R., The Mathematical Theory of Plasticity, London, Oxford University Press, 1950.

25. Drucker, D.C., "Some Implications of Work Hardening Ideal Plasticity", Quarterly, Applied Mathematics, Vol. 7, No. 4, December 1950, pp. 411-418.

Table 1: Material Properties

	Specimens 1 & 2	Specimens 3 & 4	Specimens 5 & 6
(a) Concrete			
Compressive Strength	34.2 MPa	31.7 MPa	22.7 MPa
Splitting Tensile Strength	3.5 MPa	3.3 MPa	2.7 MPa
(b) Longitudinal Reinforcement			
Number and Size	12 – No. 6	8 – No. 7	8 – No. 7
Yield Stress	454 MPa	441 MPa	464 MPa*
Ultimate Stress	782 MPa	696 MPa	689 MPa*
(c) Lateral Reinforcement			
Number and Size	3 – No. 3	1 – No. 3	1 – No. 2
Interval	127 mm	53 mm**	51 mm
Yield Stress	510 MPa	500 MPa	303 MPa

* The corner longitudinal bars were the same as
Specimens 3 & 4, and the values shown are for the
centre longitudinal bars.

** The values are for the portion within a distance
equal to twice effective depth from the footing surface.
Outside that portion the spacing is twice the value shown.
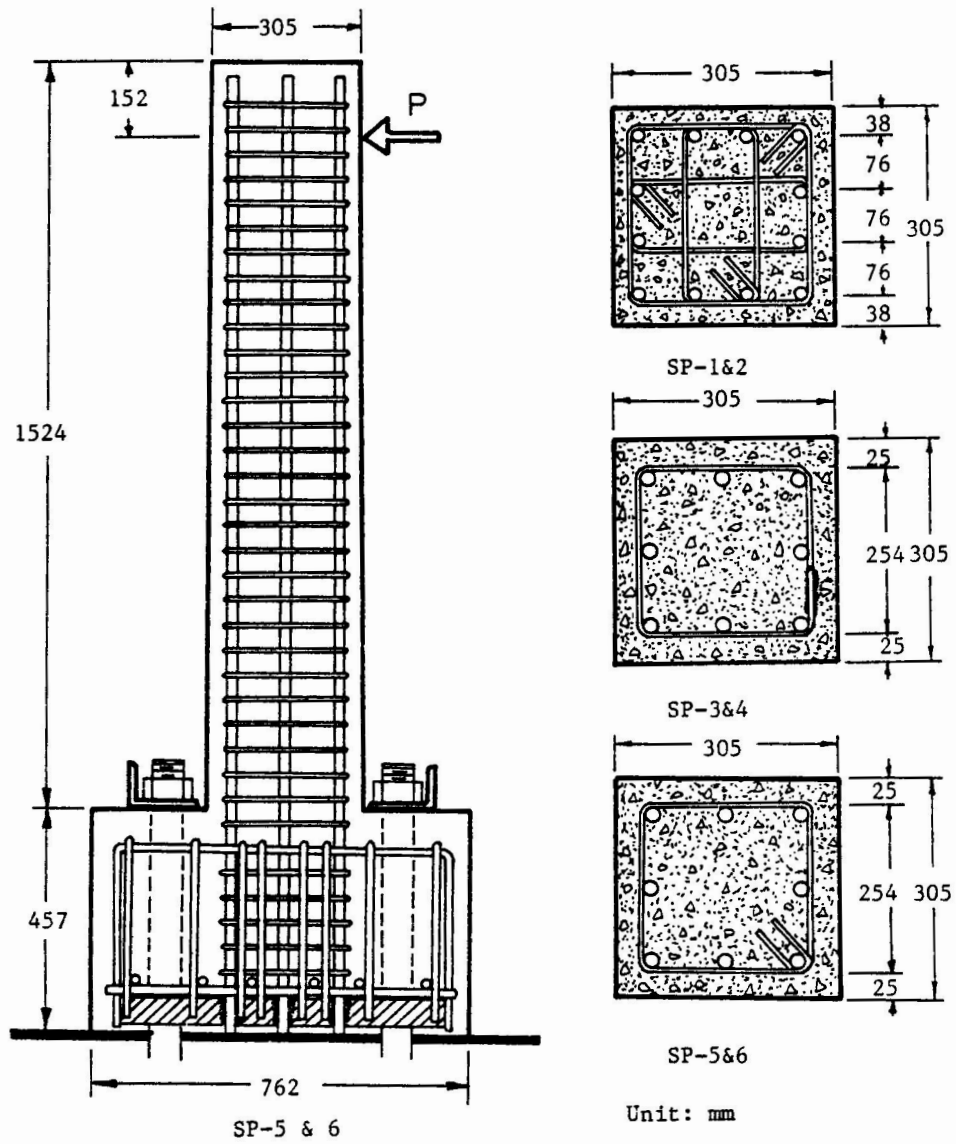
Fig. 1: Arrangement of Reinforcement in Column Specimens
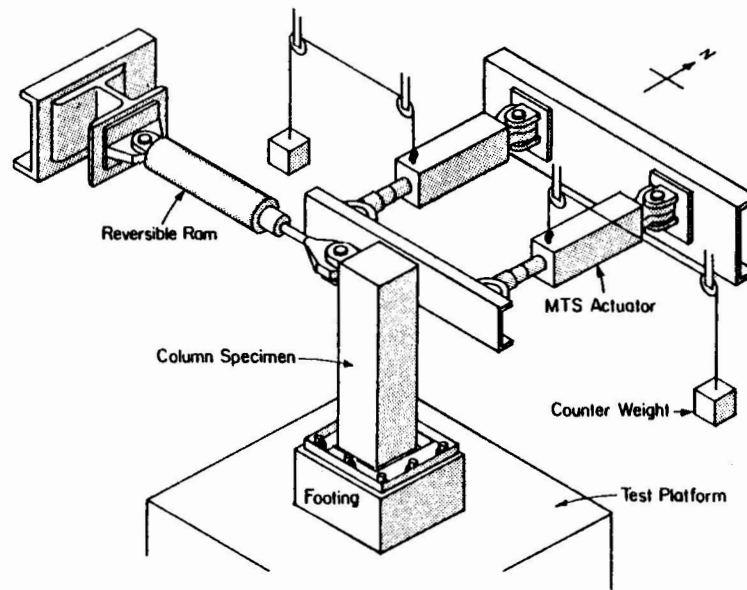
Fig. 2: Loading System for Biaxial Lateral Load Test

Observed Displacement / Calculated Yield Deflection
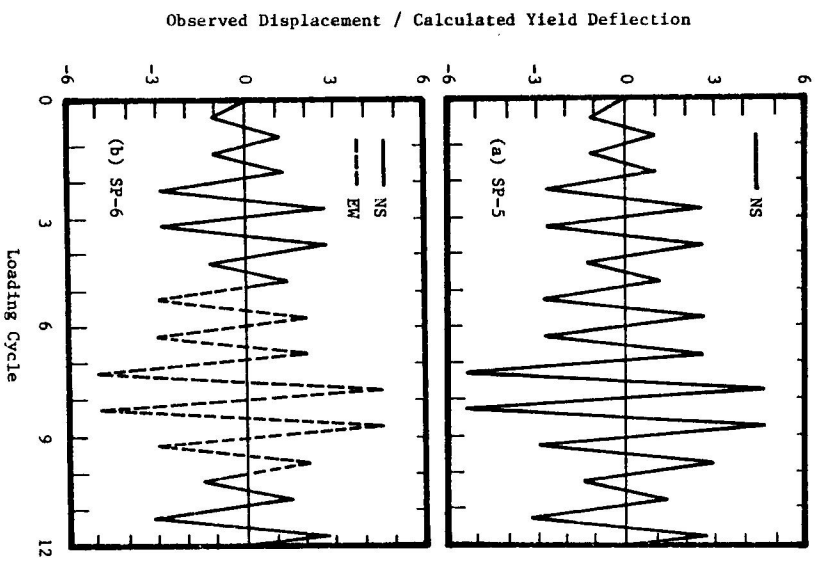
Fig. 3: Typical Loading Programs
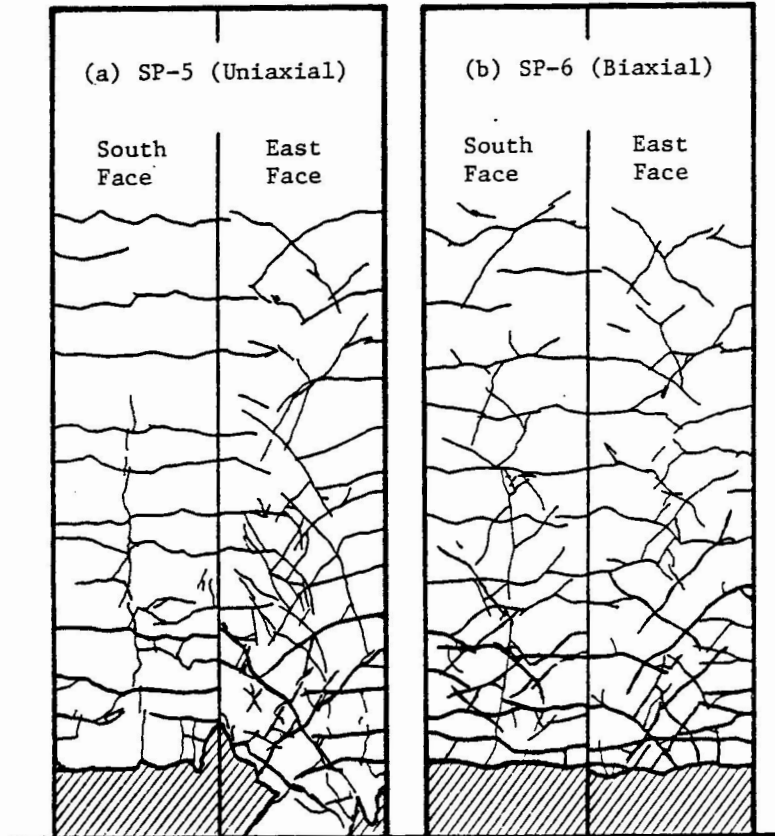
Fig. 4: Observed Crack Patterns Before Failure
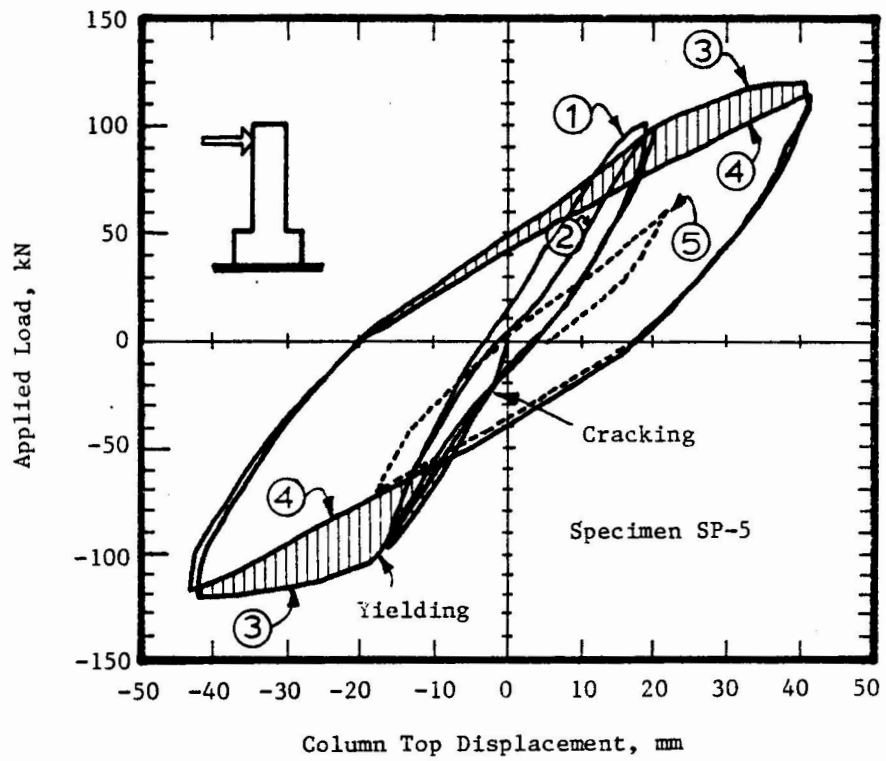
Fig. 5: Stiffness Reduction Under Uniaxial Loading
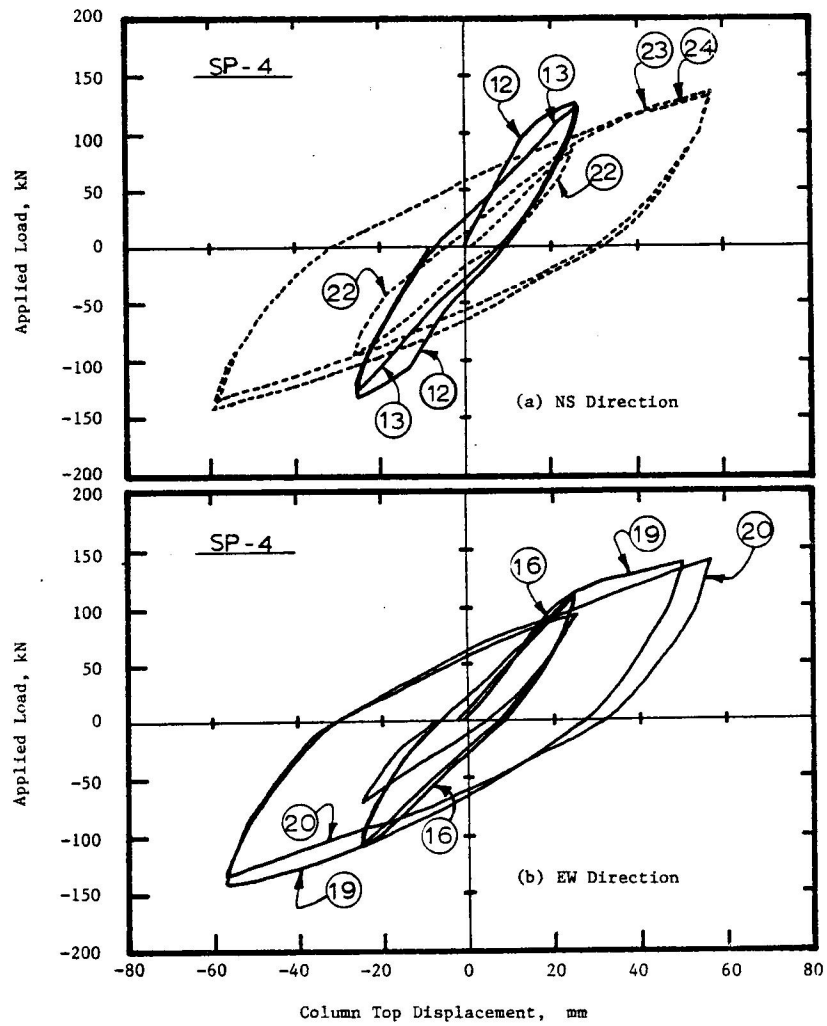
Fig. 6: Effect of Transverse Loading on Stiffness
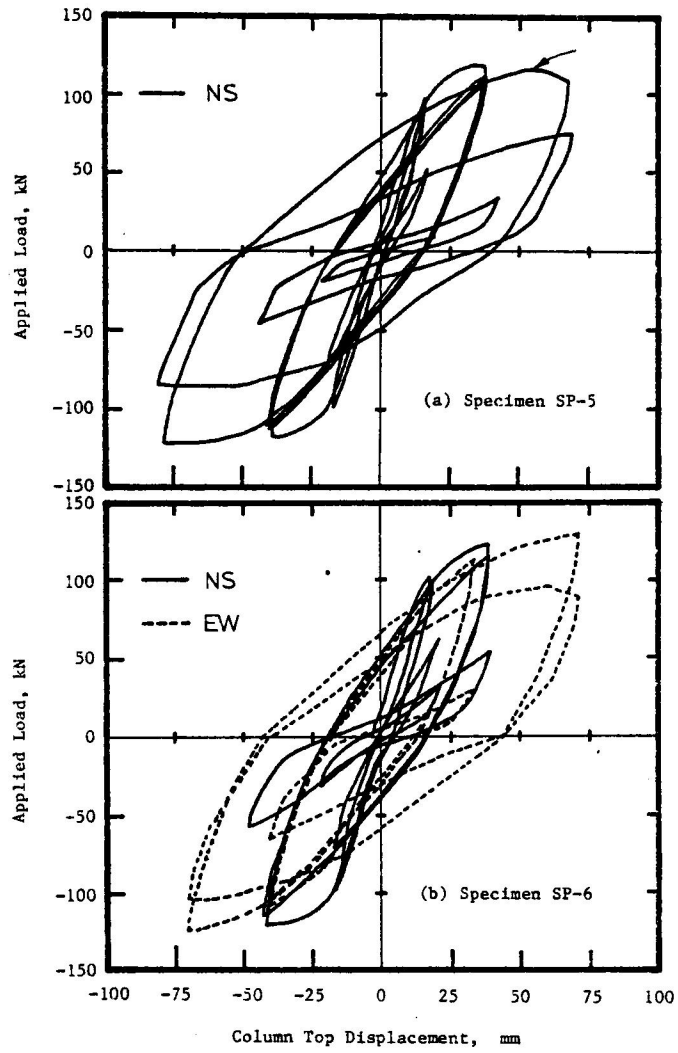
Fig. 7: Hysteretic Characteristics of Uniaxially and
Biaxially Loaded Columns
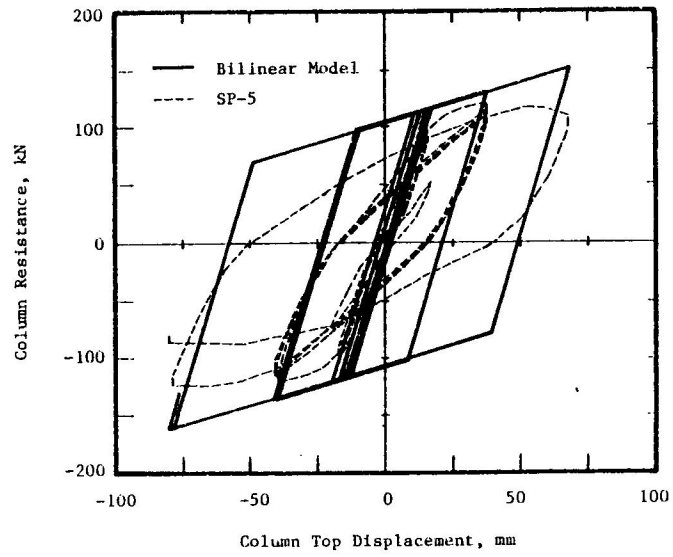
Fig. 8:   Non-Degrading Bilinear Hysteresis Model
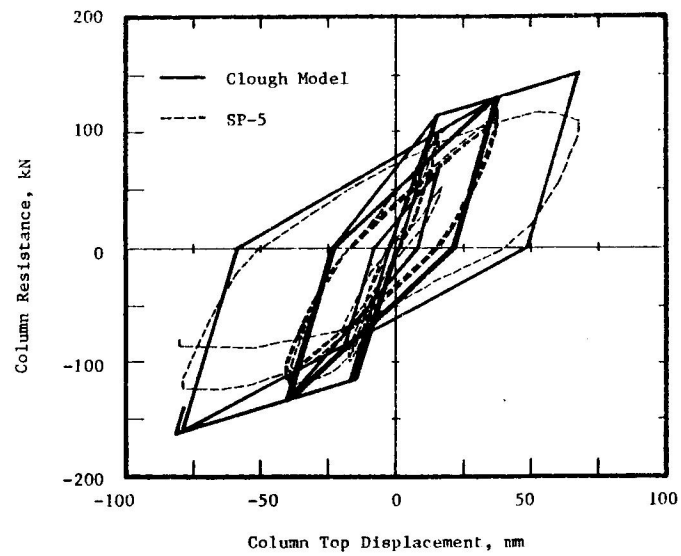
Fig. 9:   Clough's Degrading Hysteresis Model
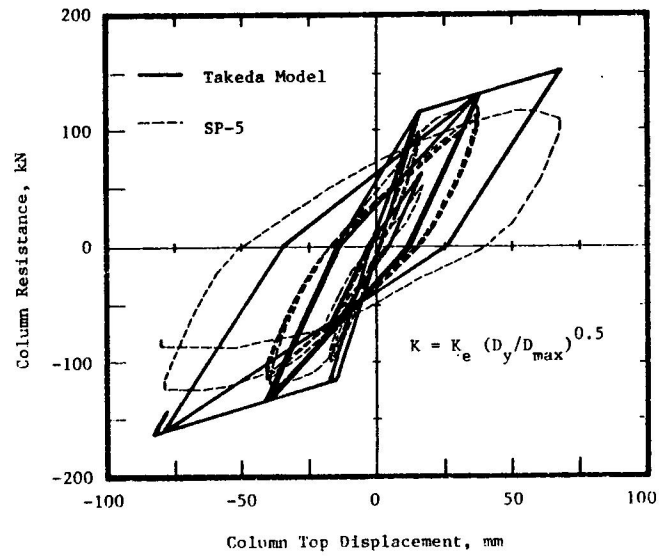
Fig. 10: Takeda's Degrading Hysteresis Model (I)

$$K = K_e \left(D_y / D_{max} \right)^{0.5}$$
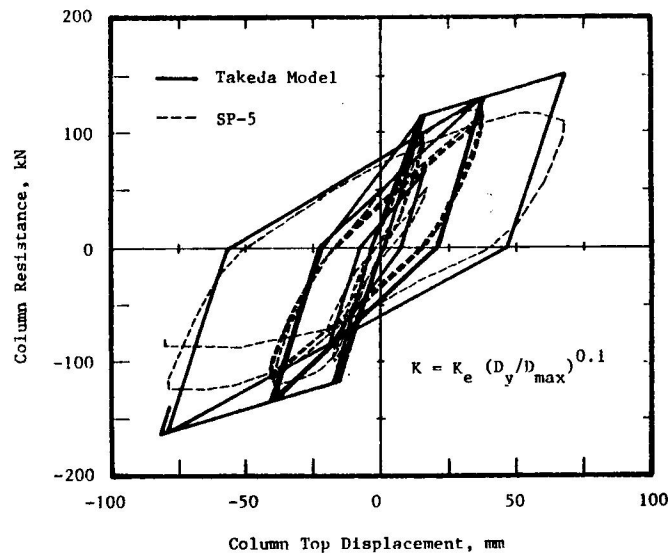
Fig. 11: Takeda's Degrading Hysteresis Model (II)

$$K = K_e \left(D_y / D_{max} \right)^{0.1}$$
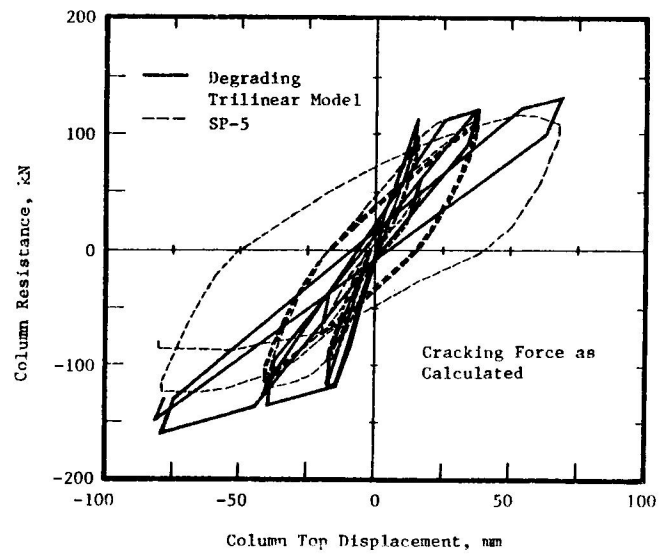
Fig. 12: Degrading Trilinear Hysteresis Model (I)
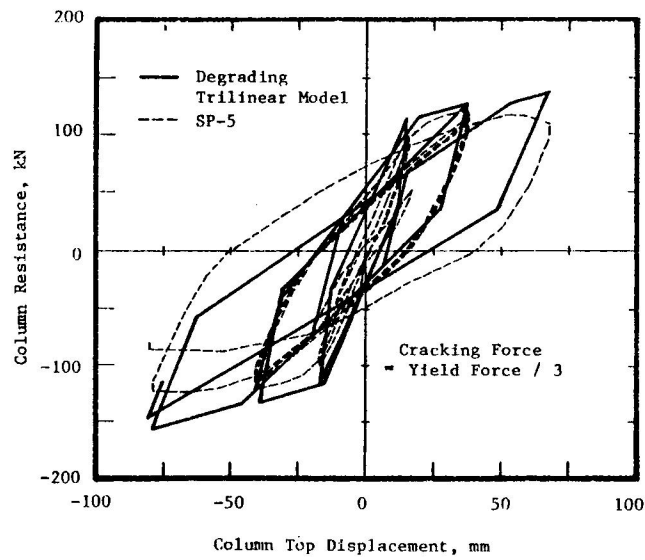
Fig. 13: Degrading Trilinear Hysteresis Model (II)
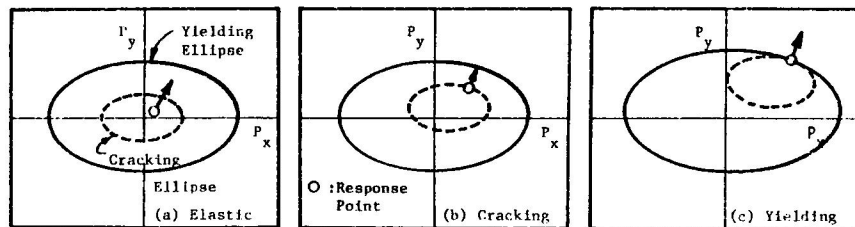
Fig. 14: Different Response Stages for Biaxial Degrading
Trilinear Model
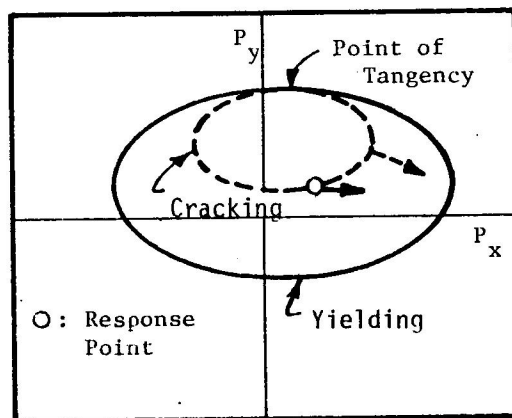
Fig. 15: Sliding of Cracking Ellipse
Along Yielding Ellipse
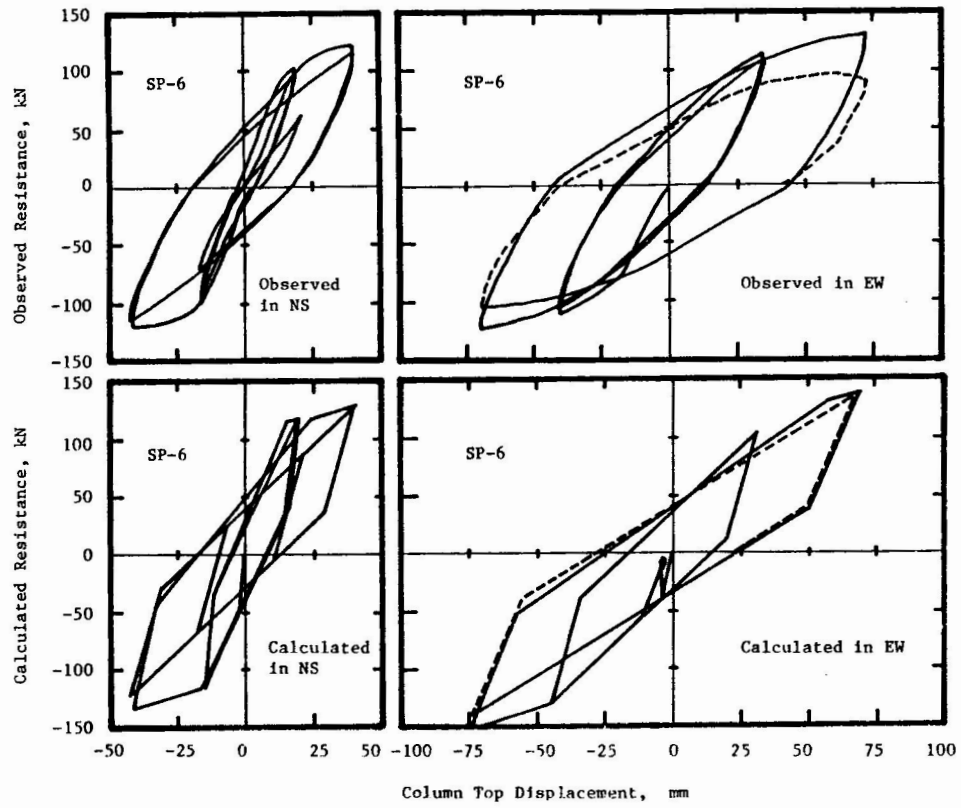
Fig. 16: Observed and Calculated (Biaxial Degrading Trilinear Model) Behaviour of Specimen SP-6